

Flexible Linker Modulates Glycosaminoglycan Affinity of Decorin Binding Protein A

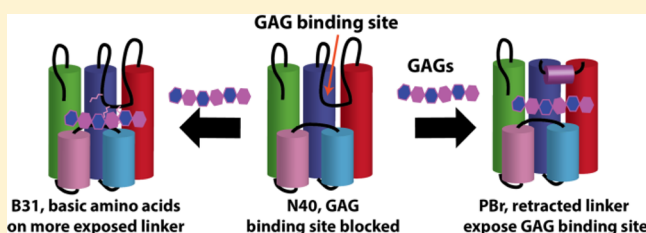
Ashli Morgan,[†] Krishna Mohan Sepuru,[‡] Wei Feng,[†] Krishna Rajarathnam,[‡] and Xu Wang^{*,†}

[†]Department of Chemistry & Biochemistry, Arizona State University, Tempe, Arizona 85287, United States

[‡]Department of Biochemistry and Molecular Biology, Sealy Center for Structural Biology and Molecular Biophysics, University of Texas Medical Branch, Galveston, Texas 77555, United States

S Supporting Information

ABSTRACT: Decorin binding protein A (DBPA) is a glycosaminoglycan (GAG)-binding adhesin found on the surface of the bacterium *Borrelia burgdorferi* (*B. burgdorferi*), the causative agent of Lyme disease. DBPA facilitates bacterial adherence to extracellular matrices of human tissues and is crucial during the early stage of the infection process. Interestingly, DBPA from different strains (B31, N40, and PBr) show significant differences in GAG affinities, but the structural basis for the differences is not clear. In this study, we show that GAG affinity of N40 DBPA is modulated in part by flexible segments that control access to the GAG binding site, such that shortening of the linker leads to higher GAG affinity when analyzed using ELISA, gel mobility shift assay, solution NMR, and isothermal titration calorimetry. Our observation that GAG affinity differences among different *B. burgdorferi* strains can be attributed to a flexible linker domain regulating access to the GAG-binding domain is novel. It also provides a rare example of how neutral amino acids and dynamic segments in GAG binding proteins can have a large influence on GAG affinity and provides insights into why the number of basic amino acids in the GAG-binding site may not be the only factor determining GAG affinity of proteins.



Decorin-binding protein (DBP) is a surface lipoprotein found on the bacterium *Borrelia burgdorferi* (*B. burgdorferi*), the causative agent of Lyme disease. DBP adheres to the connective tissue proteoglycan decorin, which allows the bacterium to be retained in the extracellular space of the host tissue.^{1,2} Studies have shown DBPs attach to decorin mainly by binding glycosaminoglycans (GAGs) on decorin.^{1,3} GAGs are linear, sulfated polysaccharides ubiquitous to all mammals. Although GAG polysaccharides contain only two types of monosaccharides, they are among the most complex biomolecules because of the semirandom modifications of these monosaccharides through epimerization and sulfation.⁴ DBPs are known to bind several GAGs. Besides dermatan sulfate (DS), the type of GAG most commonly found in decorin, DBPs also bind heparin and heparan sulfate (HS).⁵ Although all three GAGs have high levels of iduronic acid, DS alone contains N-acetylgalactosamine (GalNAc) while heparin/HS contain glucosamine (Figure 1A). DBPA's ability to bind different GAG types may be a factor in determining its tissue tropism. In fact, studies have shown DBP's affinity for various GAG types is correlated with its adherence to different host organs.^{6,7}

Two homologous forms of DBP, DBPA and DBPB, exist in the *B. burgdorferi* genome. The two homologues share about 40% sequence identity and both are crucial to the early stage infection process.^{8,9} In particular, deletion of DBPA/B genes attenuates virulence by 3 to 4 orders of magnitude.

Interestingly, whereas the sequence of DBPB is highly conserved, the sequence of DBPA is less conserved among different strains. Significance of these sequence variations lies in their effect on differences in the clinical manifestation of Lyme disease. Recent studies by Leong and co-workers showed that DBPAs from different strains have very different affinities for GAGs, and DBPA sequence alone was sufficient in determining tissue tropism of the bacterium.^{10,11} In particular, they found that transfecting bacterial strains naturally devoid of DBPA with PBr DBPA, which binds DS with a K_D 0.21 μ M, led to bacterial colonization in the heart, whereas expression of N40 DBPA, which binds DS with a K_D 3.10 μ M, resulted in localization to the knee. These results show that GAG affinity and specificity of DBPA dictate bacterium localization, and therefore understanding the molecular basis underlying DBPA–GAG interactions may lead to advanced prediction of the clinical manifestation of the disease.

So far, structures of DBPA from three different strains of *Borrelia* spirochetes have been determined.^{12,13} Despite the sequence differences, their structures are very similar. All structures contain five helices and two flexible segments. The helical bundle is stabilized by a considerable hydrophobic core, and a GAG-binding site can be found on its surface (Figure

Received: March 8, 2015

Revised: July 23, 2015

Published: July 30, 2015



		HELIX 1	LINKER	
N40	29	GLKGE ETKIILERSAKDITDEINKIKKDAADNN <u>VNFAAF</u> TDSETGSKVSEN SFILEAKVR		87
		HELIX 2	HELIX 3	HELIX 4
N40	88	ATTVAEK FVTAIEGEATK LKKTGS SGEFS AMYNM LEVSGPLEEL LGVLRL MTKT VTDAEQ		147
		HELIX 5		
N40	148	HPTTTAEGIL LEIAKIM TKLQ RVHTKN YCALEKKKNPNFTDEKCKNN		194
			*	*

Figure 2. Mutants of N40 DBPA considered in this study. Sequences of helical regions of WT N40 DBPA are highlighted in black. The mutations made in this study are indicated as follows: the three linker deletion mutations are underlined, the neutral linker mutations are shaded gray, and the disulfide bond mutation is notated with an asterisk (*). The linker deletion mutants are as follows: N40_{Δ62–66}, N40_{Δ62–71}, and N40_{Δ62–74}. The neutral linker mutants include N40_{neutral} and N40_{Δ62–71,neu}. The C-terminal disulfide bond was removed in the mutant C176S/C191S.

incubated with 2 μg of His-tagged WT N40 DBPA and N40 DBPA mutants in 100 μL PBS for 1 h. The bound protein was quantified using 1:2000 Anti-His HRP (Qiagen) and developed with tetramethylbenzidine (TMB) substrate solution. 100 μL of 0.1 M sulfuric acid was added to each well to stop the reaction after 2 min (heparin) or after 12 min (DS), inducing a color change that was read at 450 nm. Each ELISA assay was performed at least twice, and data from four replicates of every sample were averaged to obtain the mean and standard deviation.

Production of Heparin and DS Fragments. Commercially available heparin and DS were digested with either heparinase I (heparin) or chondroitinase ABC (DS) until 30% of available sites are cleaved. Digests were monitored by measuring absorbance at 232 nm to determine extent of digests. The partially depolymerized GAGs were then separated with a size exclusion chromatography column (Bio-Rad Biogel P10) to obtain homogeneous size-defined fragments.

Gel Mobility Shift Assays for N40 DBPA Variants. Heparin dp8 (degree of polymerization 8, or octasaccharide) and DS dp8 fragments were fluorescently labeled with 0.1 M 2-aminoacridone (2-AMAC) as described by Lyon et al.¹⁸ The assay was performed by incubating 2 μg of the 2-AMAC labeled heparin dp8 or DS dp8 with either 0.5 (heparin) or 1 (DS) mol equiv of DBPA in 50 mM sodium phosphate pH 6.5, 150 mM NaCl for a total volume of 12.5 μL. The reaction mixtures were incubated at RT for 30 min, and run in a 2% agarose gel at 120 V for 15–20 min. A UV panel was used to visualize the shifts.¹⁹ Quantification was carried out by comparing brightness-weighted pixel counts of the free bands in the presence and absence of the protein.

Titration of WT and Mutant N40 with Heparin dp8. ¹H–¹⁵N HSQC spectra were collected on a Bruker Ultra-Shield 600 MHz spectrometer. The NMR titration data were used to estimate *K_D* values for the interaction between heparin dp8 and the DBPA N40 variants at pH 6.5. A total of 18 mol equiv of heparin dp8 were added in aliquots of either 2 or 4 mol equiv to 400 μL of 150 μM protein. The chemical shift changes noted in each ¹H–¹⁵N HSQC spectrum were normalized into one chemical shift value using the equation, $\delta_H = [\Delta\delta_H^2 + 1.7\Delta\delta_N^2]^{1/2}$, where δ_H and δ_N represent the chemical shifts for ¹H and ¹⁵N in hertz, respectively.²⁰ The binding curves were fitted using the one-to-one binding model contained in the software xcrvfit (<http://www.bionmr.ualberta.ca/bds/software/xcrvfit/>) to extract the *K_D* values.

Isothermal Titration Calorimetry (ITC). The binding affinities of DBPA N40 variants were characterized by measuring the heat changes on titrating dp10 heparin into the DBPA solution using a Microcal VP titration Calorimeter.

Protein and GAG solutions were dissolved in 50 mM phosphate 150 mM NaCl (pH 6.5), centrifuged, and degassed under vacuum before use. Titrations were performed by injecting 2 × 2 μL and 6 × 46 μL aliquots of GAG into DBPA solution at 25 °C. Data were analyzed using Origin software supplied by Microcal.

RESULTS

To probe the role of the linker in modulating GAG affinity of DBPA, we constructed several mutants containing truncated linkers. We used WT N40 DBPA as our model because, unlike B31 and PBr DBPA, its linker is not known to contain elements that enhance GAG binding. Chemical shift perturbation analysis and paramagnetic perturbation using TEMPO-labeled heparin dp6 ligands both showed that the linker of N40 DBPA is minimally perturbed by heparin,¹³ indicating its interactions with GAG are most likely minimal. This property of N40 DBPA allows us to evaluate objectively the impact of the linker length on GAG affinity without the complication of removing additional GAG-binding residues in the process.

Figure 2 shows the mutants that were constructed for this study. Specifically, we prepared three N40 DBPA mutants with 5 (residues 62 to 66), 10 (residues 62 to 71), and 13 (residues 62 to 71) residues removed from the linker. These are designated as N40_{Δ62–66}, N40_{Δ62–71}, and N40_{Δ62–74}, respectively. Residues were chosen after the impact of linker shortening on nearby secondary structures was modeled using the program modeler²¹ to ensure the integrity of the helices is preserved. The NMR studies of the mutant N40_{Δ62–71} also showed that the integrity of helix-1 and helix-2 flanking the linker was not compromised. In particular, sequential HN–HN NOESY crosspeaks and backbone dihedral angles predicted from *Cα* and *Cβ* chemical shifts were consistent with the retention of the helical structure (Table S1). Besides the linker truncation mutants, we also engineered mutants without charged amino acids in the linker and a mutant missing the disulfide bond connecting the flexible C-terminal linker and helix 5. This disulfide bond tethers the flexible C-terminus close to the core domain and the basic pocket. However, the disulfide bond is missing in a number of DBPA sequences, including PBr DBPA. The Cys mutant (C176S/C191S) of N40 DBPA will allow us to evaluate whether the disulfide bond has any functional role in DBPA’s GAG-binding activity. There are also a number of charged amino acids in the linker of N40 DBPA (D68, E70, and K74). Removal of these amino acids may potentially influence DBPA–GAG interactions. To gauge their contributions to GAG binding, we also created a mutant having a linker of normal length, but with the three charged amino acids mutated to Ser (N40neutral), and another version of the

N40 $_{\Delta 62-71}$ mutant also containing a neutral linker (N40 $_{\Delta 62-71,neu}$).

We first tested the mutants' affinities for intact GAGs with ELISA assays that use immobilized heparin and DS as probes. In the case of immobilized heparin, mutants with shortened linkers showed a dramatic increase in binding affinity compared to the WT while C176S/C191S mutant showed a small decrease in affinity (Figure 3). We also performed ELISA using

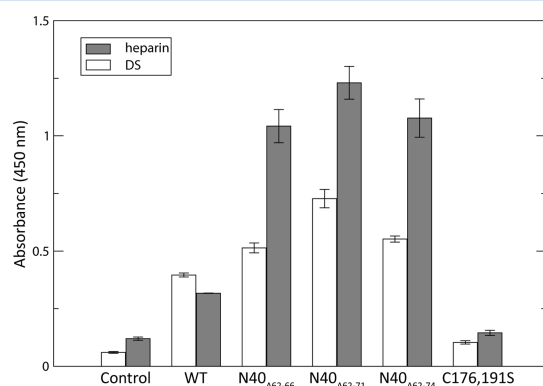


Figure 3. Effect of mutations in N40 DBPA on GAG-binding as determined by ELISA. Shortening the linker increased N40 DBPA's affinity for GAGs while removal of the C-terminal disulfide bond reduced the affinity. Student's *t* test comparing WT N40 DBPA with each mutant indicates the change in GAG-binding affinity is statistically significant ($p < 0.0001$ for both heparin and DS).

immobilized DS, the major GAG type found on decorin, as the probe. In agreement with results of the heparin ELISA, significant improvements in DS binding affinity can be seen for all linker truncation mutants (Figure 3), but the enhancements were smaller than that of heparin. These results indicate GAG affinity enhancements stemming from linker shortening may be dependent on GAG type, and this is potentially a factor in determining the preference of DBPA for tissue type. Once again, the C176S/C191S mutant showed a small but statistically significant ($p < 0.01$) decrease in DS affinity. We also carried out ELISA on mutants with neutral linkers to measure whether the enhancement in GAG affinity is the result of shortening the linker or the elimination of the charged amino acids. Figure S1 shows the result of these assays. Specifically, we saw that the mutant with normal linker length and no charged amino acids in the linker has about the same binding affinity for GAGs as WT N40 DBPA, indicating the net effect of the charged amino acids on GAGs is minimal. Shortening the linker resulted in substantial increase in both heparin and DS affinities. Specifically, N40 $_{\Delta 62-71,neu}$'s affinity of heparin increased ~ 2.5 -fold while its DS affinity doubled. These are comparable to increases seen in N40 $_{\Delta 62-71}$.

To obtain a more quantitative insight, we also probed the binding interactions using size-defined heparin and DS oligosaccharides. First, the qualitative affinities of the mutants for heparin dp8 (degree of polymerization 8, or octasaccharides) and DS dp8 were carried out using gel mobility shift assay (GMSA). The GMSA measures the extent to which a protein is capable of impeding the electrophoretic migration of fluorescently labeled GAG ligands. The results showed that the linker truncated N40 DBPA mutants have significantly higher affinity for heparin dp8 than the WT, as demonstrated by the large amount of heparin fragments whose migration the mutants have impeded (Figure 4A). On the other hand, heparin

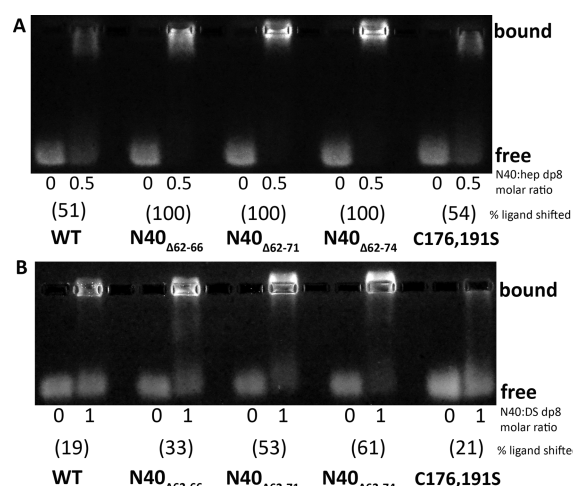


Figure 4. GMSA of heparin dp8 (A) and DS dp8 (B) in the presence of either 1 or 0.5 equiv of WT N40 DBPA and N40 $_{\Delta 62-66}$, N40 $_{\Delta 62-71}$, N40 $_{\Delta 62-74}$, and N40 C176S/C191S mutants.

affinity of the C176S/C191S mutant was no different compared to the WT. The linker mutants also significantly increased the amount of DS dp8 fragments shifted compared to the WT, but the C176S/C191S mutant did not show significant changes compared to the WT. Both are in agreement with the ELISA results. It should be noted that, because of DBPA's weaker affinity for DS, twice as much DBPA was required to shift a comparable amount of DS as heparin fragments.

We then characterized these interactions using solution NMR titrations. We used heparin dp8 as the representative GAG ligand because our previous NMR work has shown that DBPA binding to DS fragments fall within the intermediate exchange regime on the NMR time scale, preventing accurate extraction of K_D values, and GMSA data indicate that the relative heparin affinities reliably capture their affinities for DS.^{15,16} For the NMR studies, the mutants were titrated with heparin dp8, and large binding-induced chemical shift perturbations of the pocket residues (T90, T140, and R169) were measured and fitted to obtain the K_D . Figure 5 shows the chemical shift changes of T140 in WT and mutant N40 DBPA as well as the binding curves derived from these data. Table 1 summarizes the K_D s of linker truncated DBPAs. Shortening the linker decreased K_D from several mM to ~ 0.2 mM for mutants with linkers shortened by 10 residues or more. On the other hand, K_D for the disulfide bond mutant, C176S/C191S N40 DBPA, only decreased from several mM to ~ 0.8 mM. This trend in K_D values is qualitatively consistent with the GMSA results. In total, these experiments demonstrate the effect of removing the disulfide bond on N40 DBPA's GAG affinity is small.

We also determined the global binding affinities of the mutants using isothermal titration calorimetry (ITC) to independently validate K_D from the NMR experiments. The size of heparin was increased by a disaccharide to obtain a higher change in enthalpy so the K_D s can be accurately measured. Figure 6 and Table 1 summarize the result of the ITC experiments. The ITC data show that mutants with shortened linkers were able to produce significantly higher changes in enthalpy than WT or C176S/C191S N40 DBPA. Trends of K_D changes between the WT and mutants measured are also in complete agreement with GMSA and NMR titration data. Namely, mutants with shortened linkers showed

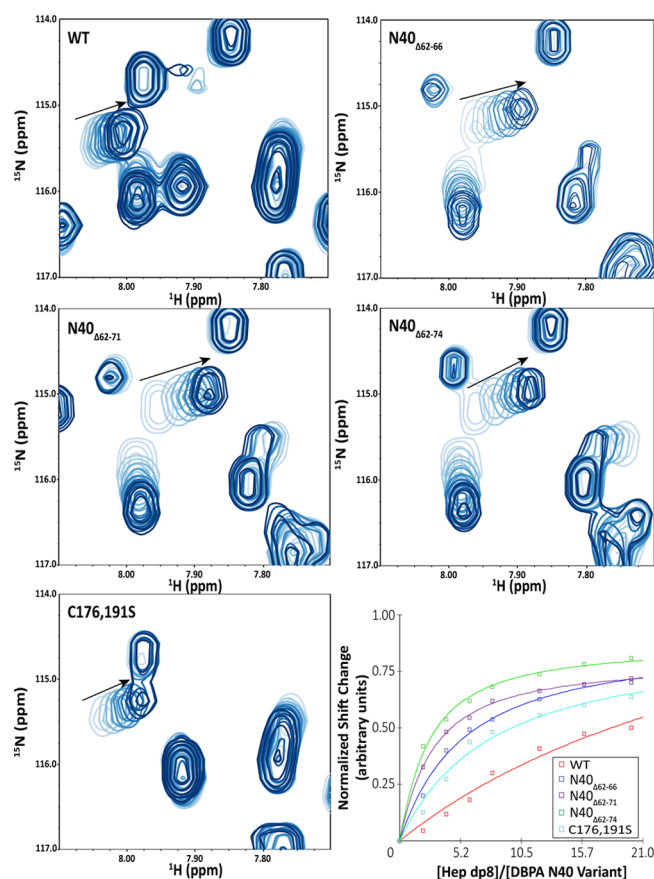


Figure 5. ^{15}N -HSQC overlays of residue T140 of N40 DBPA variants in the presence of increasing concentrations of heparin dp8. The lightest contour represents the initial HSQC spectrum of N40 in the absence of heparin dp8. Each subsequent contour represents the increasing concentrations of heparin dp8: 0.2, 0.4, 0.6, 0.8, 1.2, 1.6, and 2.0 mM. The concentration of N40 was 0.15 mM. Overlay of K_D curves for T140 of each N40 variant is shown in the bottom right panel.

Table 1. N40 Linker Mutants Show Increased Binding to Heparin Fragments (Heparin dp8 for NMR and Heparin dp10 for ITC)

N40 Variant	NMR	ITC
	K_D (μM)	K_D (μM)
WT	>2 mM	>650
N40 Δ_{62-66}	495 \pm 59	617 \pm 55
N40 Δ_{62-71}	234 \pm 11	153 \pm 7
N40 Δ_{62-74}	200 \pm 20	219 \pm 6
C176S/C191S	751 \pm 176	>650

significantly lower K_D s than the WT, and C176S/C191S N40 DBPA showed negligible change compared to the WT protein.

DISCUSSION

The results of this study show the flexible linker of DBPA is a critical negative regulator of GAG-affinity. This is consistent with our hypothesis that the linker occludes the binding pocket and reduces access of GAGs, thus reducing the protein's affinity for GAGs despite having a rich collection of basic amino acids in the pocket. Shortening the linker removes the obstruction and increases the GAG affinity. This is a novel result because conventional wisdom states that GAG affinities of GAG-

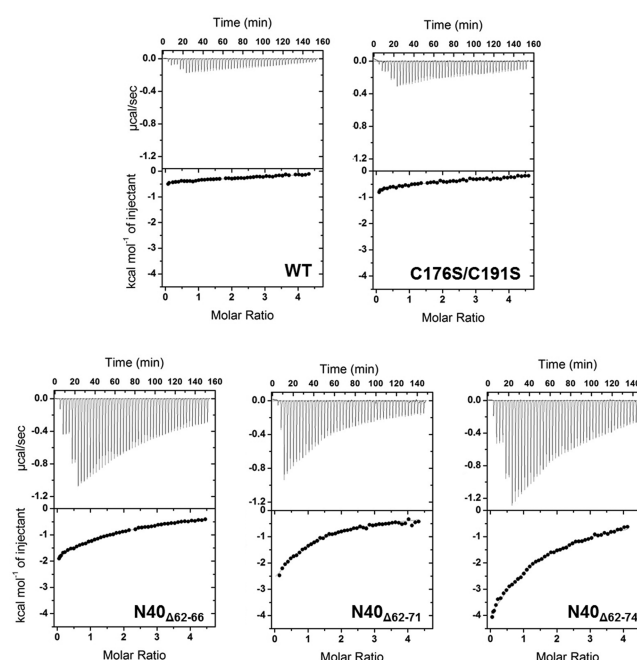


Figure 6. ITC titration curves of N40 DBPAs with heparin dp10. Values of K_D s extracted from these data are shown in Table 1.

binding proteins are controlled mostly by the number of basic amino acids in the binding site. However, residues removed in this study are not part of the binding site and the number of basic amino acids in the pocket was not altered. In addition, our results show that the GAG affinity enhancement gained from shortening the linker does not apply to all GAG types, and that linker truncation enhanced heparin binding to a much greater extent than DS binding.

These results explain much of the observed differences in GAG affinities of DBPAs from different strains. N40 DBPA, ^{10,11} whose basic pocket constitutes the only major GAG binding site, has the weakest affinity because of lack of access to the basic pocket by the ligand. B31 DBPA, on the other hand, possesses additional basic residues clustered in its linker, allowing for increased electrostatic interactions between the protein and GAGs through these more exposed residues. PBr DBPA evolved an alternate strategy to overcome the barrier of occluded GAG-binding site by having a helical linker, whose compact shape allows the pocket to be much more exposed and accessible for interactions with GAGs. Considering PBr DBPA shows higher affinity for heparin-like GAGs than N40 or B31 DBPAs, these differences in affinity may be a factor in determining tissue tropism during infection. Knowing the mechanisms that regulate GAG affinities could therefore allow more accurate prediction of how GAG-DBPA interactions determine localization of Lyme disease.

The fact that the linker residues occlude the basic pocket does not mean the basic residues in the pocket do not play a role in GAG binding. Indeed, previous studies have shown that mutating these residues to serine reduced GAG affinity. ^{12,14,15} These residues can contribute to GAG binding through at least two mechanisms: first, because electrostatic interactions are long-range, the presence of these residues in the vicinity may be sufficient to attract GAGs without direct contact, the protein-GAG complex can then be stabilized through formation of hydrogen bonds with polar residues in the linker; second, the large size of most native GAG chains means multivalent

interactions between DBPA and GAGs will significantly enhance affinity in vivo. It also should not be surprising that evolutionary pressures have not managed to produce a DBPA with a more efficient GAG-binding mechanism. Higher GAG affinity does not imply more efficient colonization. Biological processes such as bacterial infection are usually fine-tuned to achieve an optimal level of interactions to allow adhesion to host without attenuating proper dissemination. Furthermore, even though these proteins' affinity for GAG is weakened, through avidity effects, they may still produce sufficient adherence to prevent the bacterium from being cleared from the host tissue. Other GAG-binding adhesins may also be in place to compensate for DBPAs' weaker affinity, thus reducing the pressure on the bacterium to generate a more efficient GAG adhesin.

GAG-binding proteins constitute an important class of proteins that control critical biological phenomena such as leukocyte trafficking, blood coagulation, and cancer cell metastasis.^{22,23} Because of their importance, there has always been an interest in understanding factors determining these proteins' specificity and affinity for GAGs. However, high resolution structural information on these systems is scarce because of the dynamic nature of these interactions and heterogeneity existing in the GAG ligands. Available structural data show that GAG-binding sites in these proteins adopt diverse conformations and have little sequence homology. Although most of these sites are enriched in basic amino acids, the number of basic amino acids in the binding site is not always a good predictor of the binding affinity.⁵ Our current work presented here shows that GAG affinities can also be regulated by linker domains functioning as flaps. As far as we know, DBPA is the only reported example of a protein regulating GAG affinity using such a mechanism. However, given the prevalence of unstructured loops in GAG-binding proteins, more proteins with such a regulatory mechanism may be identified in the future.

■ ASSOCIATED CONTENT

Supporting Information

The Supporting Information is available free of charge on the ACS Publications website at DOI: 10.1021/acs.biochem.5b00253.

Information on dihedral angles of residues surrounding the linker of N40_{Δ62–71} and heparin/DS ELISA results of wild type N40 and mutants with neutral linkers (PDF)

■ AUTHOR INFORMATION

Corresponding Author

*E-mail: xuwang@asu.edu. Phone: (480)727-8256.

Funding

Funding for this study was provided by National Institutes of Health grants R00GM088483 (X.W.) and P01 HL107152 (K.R.).

Notes

The authors declare no competing financial interest.

■ ACKNOWLEDGMENTS

We thank Dr. Brian Cherry of Magnetic Resonance Research Center at Arizona State University for maintenance of the spectrometers.

■ ABBREVIATIONS

DBP, decorin-binding protein; DBPA, decorin-binding protein A; DBPB, decorin-binding protein B; DS, dermatan sulfate; ELISA, enzyme-linked immunosorbent assay; GAG, glycosaminoglycan; GMSA, gel mobility shift assay; HS, heparan sulfate; HSQC, heteronuclear single quantum coherence; ITC, isothermal titration calorimetry; NMR, nuclear magnetic resonance

■ REFERENCES

- (1) Guo, B. P., Brown, E. L., Dorward, D. W., Rosenberg, L. C., and Hook, M. (1998) Decorin-binding adhesins from *Borrelia burgdorferi*. *Mol. Microbiol.* 30, 711–723.
- (2) Guo, B. P., Norris, S. J., Rosenberg, L. C., and Hook, M. (1995) Adherence of *Borrelia burgdorferi* to the proteoglycan decorin. *Infection and immunity* 63, 3467–3472.
- (3) Fischer, J. R., Parveen, N., Magoun, L., and Leong, J. M. (2003) Decorin-binding proteins A and B confer distinct mammalian cell type-specific attachment by *Borrelia burgdorferi*, the Lyme disease spirochete. *Proc. Natl. Acad. Sci. U. S. A.* 100, 7307–7312.
- (4) Varki, A. (2009) *Essentials of glycobiology*, 2nd ed., Cold Spring Harbor Laboratory Press, Cold Spring Harbor, N.Y.
- (5) Xu, D., and Esko, J. D. (2014) Demystifying heparan sulfate-protein interactions. *Annu. Rev. Biochem.* 83, 129–157.
- (6) Leong, J. M., Robbins, D., Rosenfeld, L., Lahiri, B., and Parveen, N. (1998) Structural requirements for glycosaminoglycan recognition by the Lyme disease spirochete, *Borrelia burgdorferi*. *Infection and immunity* 66, 6045–6048.
- (7) Leong, J. M., Wang, H., Magoun, L., Field, J. A., Morrissey, P. E., Robbins, D., Tatro, J. B., Coburn, J., and Parveen, N. (1998) Different classes of proteoglycans contribute to the attachment of *Borrelia burgdorferi* to cultured endothelial and brain cells. *Infection and immunity* 66, 994–999.
- (8) Shi, Y., Xu, Q., McShan, K., and Liang, F. T. (2008) Both decorin-binding proteins A and B are critical for the overall virulence of *Borrelia burgdorferi*. *Infection and immunity* 76, 1239–1246.
- (9) Blevins, J. S., Hagman, K. E., and Norgard, M. V. (2008) Assessment of decorin-binding protein A to the infectivity of *Borrelia burgdorferi* in the murine models of needle and tick infection. *BMC Microbiol.* 8, 82.
- (10) Benoit, V. M., Fischer, J. R., Lin, Y. P., Parveen, N., and Leong, J. M. (2011) Allelic variation of the Lyme disease spirochete adhesin DbpA influences spirochetal binding to decorin, dermatan sulfate, and mammalian cells. *Infection and immunity* 79, 3501–3509.
- (11) Lin, Y. P., Benoit, V., Yang, X., Martinez-Herranz, R., Pal, U., and Leong, J. M. (2014) Strain-Specific Variation of the Decorin-Binding Adhesin DbpA Influences the Tissue Tropism of the Lyme Disease Spirochete. *PLoS Pathog.* 10, e1004238.
- (12) Fortune, D. E., Lin, Y. P., Deka, R. K., Groshong, A. M., Moore, B. P., Hagman, K. E., Leong, J. M., Tomchick, D. R., and Blevins, J. S. (2014) Identification of lysine residues in the *Borrelia burgdorferi* DbpA adhesin required for murine infection. *Infect. Immun.* 82, 3186–3198.
- (13) Morgan, A. M., and Wang, X. (2015) Structural mechanisms underlying sequence-dependent variations in GAG affinities of decorin binding protein A, a *Borrelia burgdorferi* adhesin. *Biochem. J.* 467, 439–451.
- (14) Pikas, D. S., Brown, E. L., Gurusiddappa, S., Lee, L. Y., Xu, Y., and Hook, M. (2003) Decorin-binding sites in the adhesin DbpA from *Borrelia burgdorferi*: a synthetic peptide approach. *J. Biol. Chem.* 278, 30920–30926.
- (15) Morgan, A., and Wang, X. (2013) The novel heparin-binding motif in decorin-binding protein A from strain B31 of *Borrelia burgdorferi* explains the higher binding affinity. *Biochemistry* 52, 8237–8245.
- (16) Wang, X. (2012) Solution structure of decorin-binding protein A from *Borrelia burgdorferi*. *Biochemistry* 51, 8353–8362.

- (17) Catanzariti, A. M., Soboleva, T. A., Jans, D. A., Board, P. G., and Baker, R. T. (2004) An efficient system for high-level expression and easy purification of authentic recombinant proteins. *Protein Sci.* 13, 1331–1339.
- (18) Lyon, M., Deakin, J. A., Lietha, D., Gherardi, E., and Gallagher, J. T. (2004) The Interactions of Hepatocyte Growth Factor/Scatter Factor and Its NK1 and NK2 Variants with Glycosaminoglycans Using a Modified Gel Mobility Shift Assay. *J. Biol. Chem.* 279, 43560–43567.
- (19) Seo, E. S., Blaum, B. S., Vargues, T., De Cecco, M., Deakin, J. A., Lyon, M., Barran, P. E., Campopiano, D. J., and Uhrin, D. (2010) Interaction of human beta-defensin 2 (HBD2) with glycosaminoglycans. *Biochemistry* 49, 10486–10495.
- (20) Farmer, B. T., 2nd, Constantine, K. L., Goldfarb, V., Friedrichs, M. S., Wittekind, M., Yanchunas, J., Jr., Robertson, J. G., and Mueller, L. (1996) Localizing the NADP⁺ binding site on the MurB enzyme by NMR. *Nat. Struct. Biol.* 3, 995–997.
- (21) Sali, A., and Blundell, T. L. (1993) Comparative protein modelling by satisfaction of spatial restraints. *J. Mol. Biol.* 234, 779–815.
- (22) Conrad, H. E. (1998) *Heparin-binding proteins*, Academic Press, San Diego.
- (23) Lindahl, U., and Kjellen, L. (2013) Pathophysiology of heparan sulphate: many diseases, few drugs. *J. Intern. Med.* 273, 555–571.